Supplement of Aerosol Research, 2, 199–206, 2024
https://doi.org/10.5194/ar-2-199-2024-supplement

AEROSOL Research
Open Access

Supplement of

Reduced particle composition dependence in condensation particle counters

Peter J. Wlasits et al.

Correspondence to: Dominik Stolzenburg (dominik.stolzenburg@tuwien.ac.at)

Property	Unit	n-Butanol	Propylene Glycol
Molecular Weight [1]	$g \cdot mol^{-1}$	74.1	76.1
Surface Tension at 20 °C [2]	$N \cdot m^{-1}$	0.024	0.039
Dynamic Viscosity at 20 °C [1]	$\cdot 10^{-3}$ Pa·s	2.6	28.1
Vapor Pressure at 45 °C [3]	hPa	34.20	1.29

[1] Iida, K. et al., Aerosol Sci Technol.,43, 81-96, https://doi.org/10.1080/02786820802488194, 2008.

[2] Magnusson, L.E. et al., J. Phys. Chem. Ref. Data, 32, 1387-1410, https://doi.org/10.1063/1.1555590, 2003.

[3] Linstrom, P. J., and Mallard,W. G., Eds., NIST Chemistry WebBook, NIST Standard Reference Database Number 69, National Institute of Standards and Technology, Gaithersburg MD, 20899, https://doi.org/10.18434/T4D303, retrieved Dec. 4th, 2023.

Table S1: Properties of Working Fluids. The table summarizes molecular weight, surface tension, viscosity and vapor pressure for n-butanol and propylene glycol. The vapor pressures were calculated using Antoine's equation and the parameters found in the NIST database.

Material	CAS Reg. Nr.	Grade	Manufacturer
Ag	7440-22-4	wool for elemental analysis	Merck KGaA, Darmstadt, Germany
NaCl	-	pro analysi	Merck KGaA, Darmstadt, Germany
$(NH_4)_2SO_4$	-	pro analysi	Merck KGaA, Darmstadt, Germany
$C_{15}H_{24}$	87-44-5	≥80 %	Sigma Aldrich, St. Louis, USA

Table S2: Particle materials. The table presents the CAS registry numbers, grades and manufacturers of the chemicals used for seed particle generation.

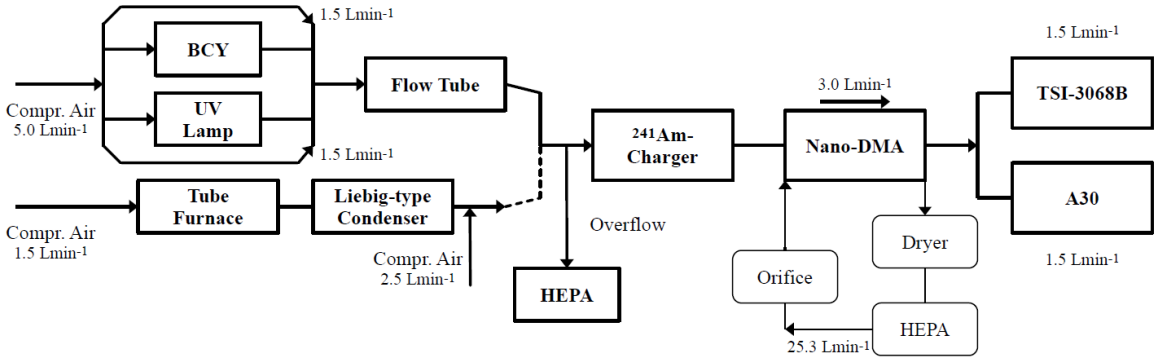

Figure S1: Schematic of the experimental setup. The experimental approach in use follows the description in Wlasits et al. (2020): Seeds originating from β-caryophyllene (BCY) were produced by ozonolysis in a makeshift flow tube. All other particle materials were evaporated in a tube furnace (Carbolite Gero GmbH & Co. KG, Neuhausen, Germany). Either of these production methods relied on compressed air as carrier gas. The carrier gas was kept dry at all times using silica gel. Downstream of the particle generators the aerosol is brought into a stable charging state using a ^{241}Am neutralizer. In a subsequent step, a Vienna-type nano-DMA classified negatively charged particles based on their electrical mobility. The size selected aerosol was then split symmetrically and fed into an FCE (TSI 3068B, TSI Inc., Shoreview, USA) and a CPC (A30, Airmodus Ltd., Helsinki, Finland).

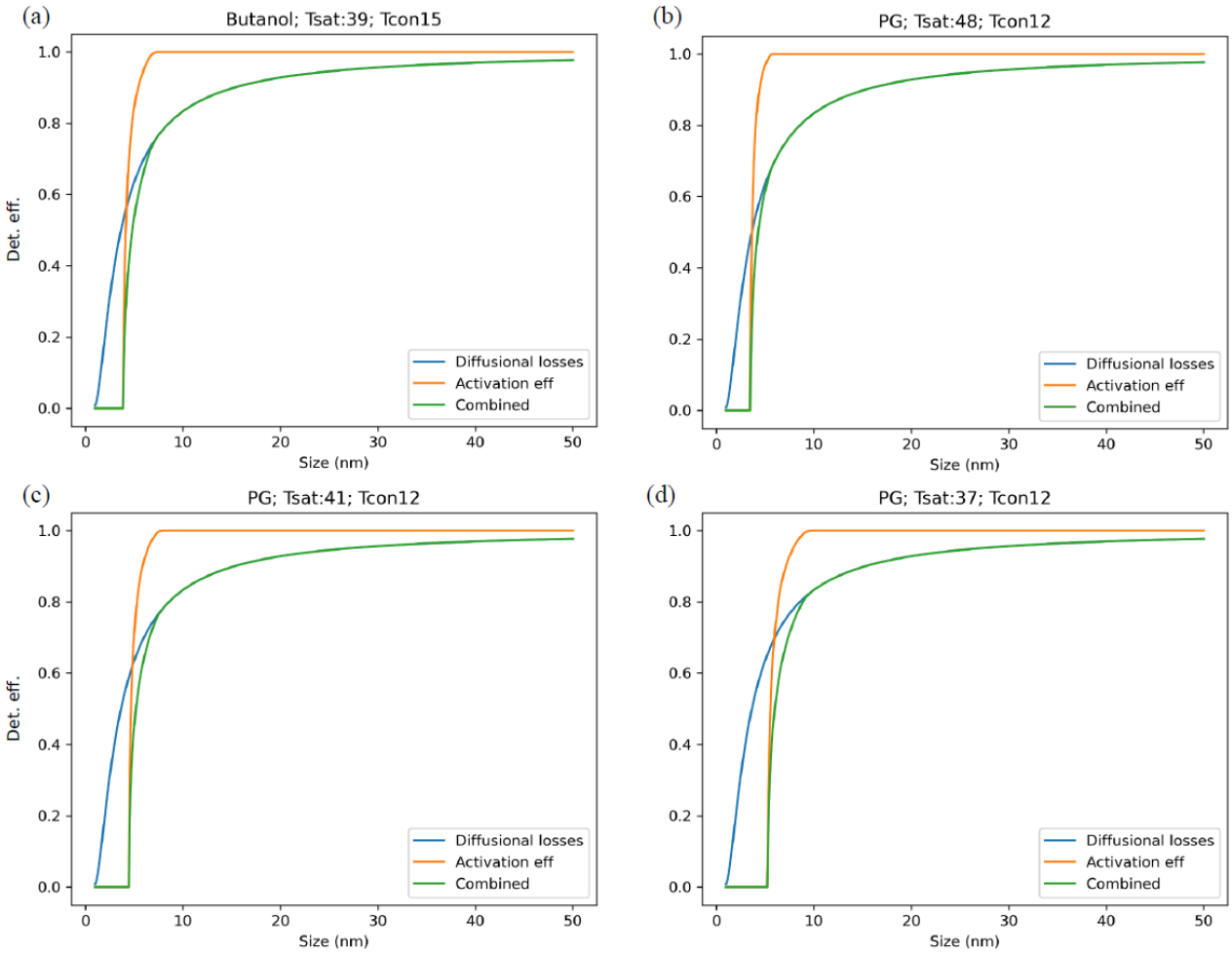

Figure S2: Detection efficiency and particle size. The figure presents the detection efficiencies for both CPCs in use as a function of the seed particle size. Each panel shows the calculated transmission efficiency based upon diffusional losses, the calculated activation efficiency as well as a curve combining both predictions. Panel (a) presents data for the butanol-based A30; panels (b)-(d) highlight the results for the propylene glycol-based CPC at three different temperature settings.

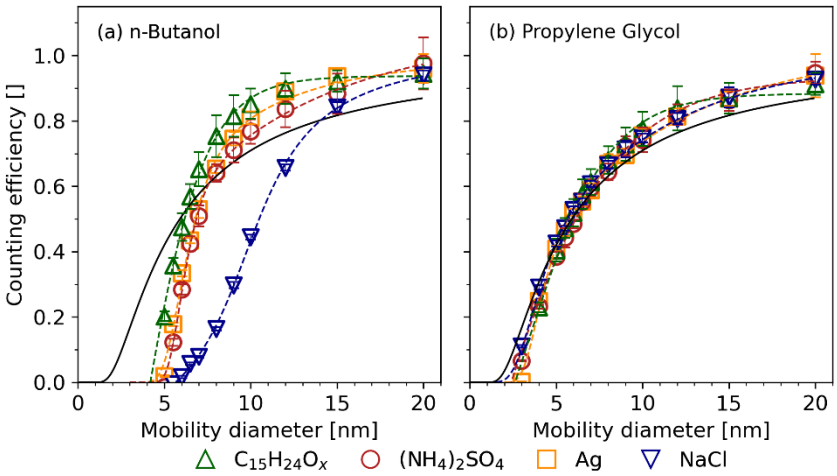

Figure S3: Counting efficiencies for butanol and propylene glycol. The figure presents the measured counting efficiencies as function of the mobility equivalent diameters. Panel (a) shows data measured with the butanol-based A30; panel (b) presents the results for the propylene glycol-based A30. Both CPCs were operated with default temperature settings. The depicted markers correspond to different seed particles. The solid black line depicts the particles' transmission efficiency according to Gormley and Kennedy (1949) with effective lengths increased by a factor of 2.6.

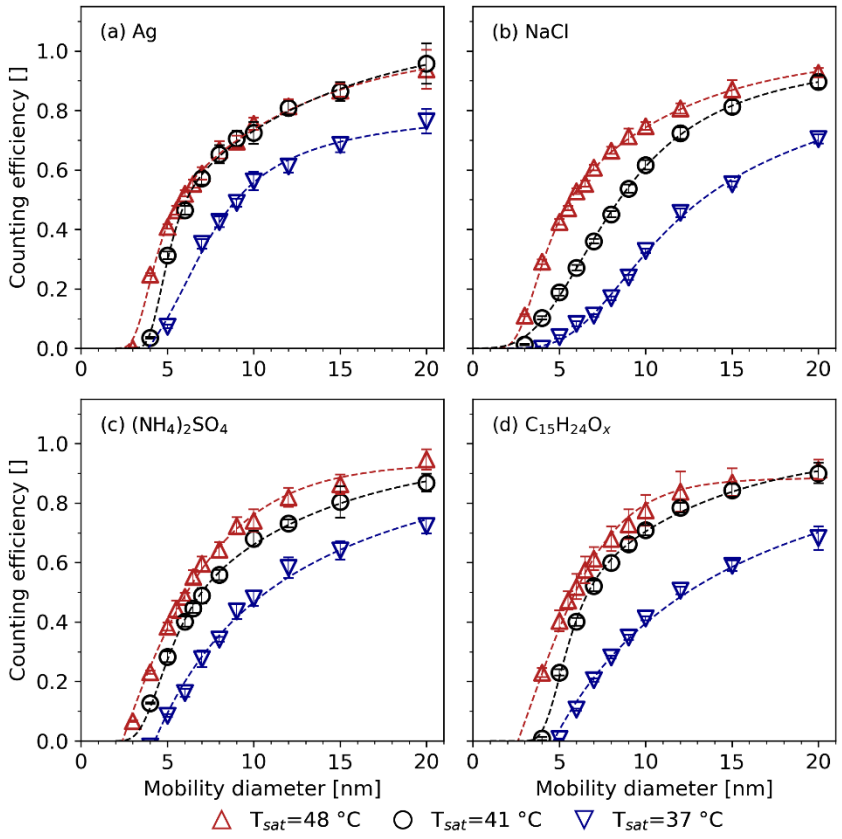

Figure S4: Counting efficiencies for default and decreased saturator temperatures. The figure shows the determined counting efficiencies as function of the mobility diameter measured using the propylene glycol-based CPC. Every panel corresponds to one of the four seed particles. The markers depict the different saturator temperatures.

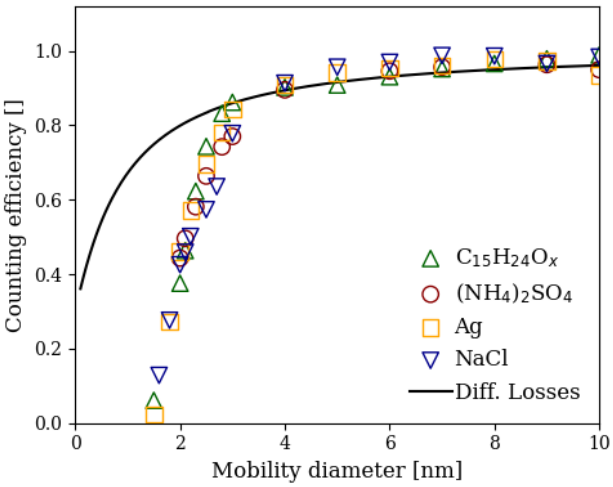

Figure S5: Counting efficiencies for the modified TSI Model 3776 (3776^T) CPC as reported in Wlasits et al. (2020), measured with the same setup as used in this study. The plateau height was slightly corrected to 1 (divided by 1.07, taken from the measurements at 20 and 30 nm with NaCl, which apparently showed unphysical values above unity). The figure presents the measured counting efficiencies as function of the mobility equivalent diameters and the depicted markers correspond to different seed particles. The solid black line depicts the particles' transmission efficiency according to Gormley and Kennedy (1949) with an effective length of 1.4 cm (0.05 L min^{-1} flow). These values are the dimension and flows for the aerosol capillary (Stolzenburg and McMurry, 1991), where the most important diffusional losses occur (due to the low flow). While the losses describe the counting efficiency curve above 4 nm reasonably well, the sharp drop of counting efficiency below 3 nm demonstrates that the diffusional losses are not the limiting factor in the TSI 3776^T for the counting efficiency below 3 nm.